

Concurrent processes in the time-resolved solvation and Coulomb ejection of sodium ions in helium nanodroplets

Florent Calvo^{1, a)}

Université Grenoble Alpes, CNRS, LIPHY, F38000 Grenoble, France

(Dated: 26 September 2024)

Recent pump-probe experiments [Albrechtsen *et al.*, *Nature* **623**, 319 (2023)] have explored the gradual solvation of sodium cations in contact with helium nanodroplets, using a fully solvated xenon atom as a probe exerting a repulsive interaction after its own ionization. In this Communication we computationally examine by means of atomistic ring-polymer molecular dynamics the mechanisms of successive ionizations, shell formation, and Coulomb ejection that all take place within tens of picoseconds, and show that their interplay subtly depends on the time delay between the two ionizations but also on the droplet size. The possibility of forming solvated Na^+Xe non-covalent complexes under a few tens of picoseconds in such experiments is ruled out based on fragment distributions.

Ion solvation is an essential process in chemical physics, involved in very diverse areas such as atmospheric and biological sciences.¹ While its main features at equilibrium are well captured in bulk environments through macroscopic concepts, monitoring the stepwise formation of solvation shells has remained a formidable challenge for experimentalists until the last decades. In a recent laser experiment, helium nanodroplets (HNDs) were used as a solvation medium, hosting impurities whose different behavior could be exploited to monitor, in real time, gradual shell formation around the first ionized impurity.² HNDs have been employed since the 1990s as a cryogenic medium enabling high resolution spectroscopic studies of various atomic or molecular dopants,^{3–6} but also, for themselves, as a probe of strongly collective quantum effects such as superfluidity. In the aforementioned experiment, the helium droplets were initially doped with both heliophobic (sodium) and heliophilic (xenon) atoms, subsequently ionized with ultrashort lasers and the ejection of the partially solvated alkali ion caused by the Coulomb repulsive force between the ions was monitored by mass spectrometry coupled with velocity map imaging. A wealth of invaluable details were thus inferred from those measurements about the rate at which helium atoms are initially captured by the newly formed ion.

The experiment of Stapelfeldt and coworkers, which provides a rather direct observation of time-resolved ion solvation in helium droplets, follows earlier attempts at monitoring the same process from spectroscopy.⁷ It was complemented by dedicated computational modeling using a continuum description of the droplet and its dynamical evolution upon sodium ionization based on the time-dependent helium density-functional theory (TD-DFT) approach⁸ and semiclassical dynamics. This model confirmed the generic picture of fast capture of the helium atom by the newborn ion under the observed time scale but with limited submersion for 2000-atom droplets. Applied to ions other than Na^+ , the TD-DFT method found

the extent of submersion to be quite dependent on the ion itself,^{7,9,10} some ions like Cs^+ being notably predicted to not even sink into 1000-atom droplets,⁷ although they readily do into He_{2000} .¹⁰ In superfluid droplets, successful submersion is also expected to produce an oscillatory motion with a period of several tens of picoseconds due to the reduced energy dissipation once the snowball is formed.⁹

In an earlier contribution,¹¹ a fully atomistic approach was employed to model the submersion process of Na^+ and Na_2^+ into small droplets containing at most several hundreds of helium atoms, the solvation and sinking time scales being inferred from the variations of appropriate time autocorrelation functions. The ring-polymer molecular dynamics (RPMD) method, which is based on Feynman's description of quantum statistics extended to the evaluation of time correlation functions,¹² was employed out of equilibrium^{13–16} to capture the same mechanisms at play during the early solvation process. It was there suggested that the solvation shell is formed concomitantly with the sinking of the sodium cation to the center of the droplet, predicted to take about 15 ps for the 500-atom droplet, both the solvation and submersion times extending markedly for the Na_2^+ impurity.¹¹ No oscillatory motion was found under the normal fluid conditions assumed in this work.

In the present Communication, and in closer relation to the experiment of Albrechtsen *et al.*,² we extend this computational effort to more realistic droplet sizes of 1000–5000 atoms and address the specific role of the xenon dopant, before and after its ionization. The simulations consist of three stages. First, the droplets containing neutral sodium and xenon impurities with prescribed numbers of helium atoms are thermalized using standard path-integral MD with massive Nosé-Hoover thermostatting. At time zero, the sodium atom is suddenly ionized, no complex multiphoton processes being at play for sodium in the experiment.² The dynamics following sudden ionization is monitored in real time by RPMD, including the local environment of the ion but also its location relative to the still neutral xenon atom. The third stage consists in ionizing the xenon dopant, a process

^{a)}Electronic mail: florent.calvo@univ-grenoble-alpes.fr

which in the experiment is multiphotonic owing to the much higher ionization potential of this element. Because we mainly monitor the sodium cation and are not especially interested in the local rearrangement in the vicinity of the xenon atom undergoing ionization, we simplify the modeling and assume again that Xe^+ is formed suddenly at a controlled time delay δt after the sodium atom.

The PIMD and RPMD methodologies employed here are well known to be approximate in several respects, starting with the neglect of exchange effects that are important in helium droplets below the superfluid temperature of 0.4 K. Extensions to incorporate such effects have been proposed in the literature^{17,18} but they remain involved or simply incompatible with any dynamical treatment of the nuclear degrees of freedom, a feature which is precisely essential here. Acknowledging this limitation, and also alleviating a significant portion of the computational cost, the initial temperature of the droplets was fixed above 0.4 K, namely 1 K for He_{1000} and He_{2000} droplets and 2 K for He_{5000} , leading to normal fluids in which nuclear delocalization is accounted for. The second major approximation is the use of RPMD for out-of-equilibrium dynamics, since the system changes potential energy surfaces twice with each ionization process. Despite important progress in path-integral methods for time correlation functions, also away from equilibrium,^{13–16,19} it is clear that the quantum dynamics they describe remains valid at short times and that only semi-quantitative details can be reasonably described with this approach.

To cope with the rather large sizes of the droplets, simplified but efficient potentials were used to describe the interactions in the NaXe@He_n , $\text{Na}^+\text{Xe@He}_n$, and $\text{Na}^+\text{Xe}^+\text{@He}_n$ systems, with parameters chosen to reproduce available reference data. More precisely, simple Lennard-Jones (LJ) interactions were employed in the neutral system for all pairs, namely He-He, Na-He, Xe-He, and Na-Xe. In the singly cationic case (Na^+ and neutral Xe), the interactions with the ions comprised an additional contribution accounting for the ion-induced dipole, either as a simple pair term ($-\alpha_{\text{Xe}}/2r^2$) for the interaction between Na^+ and He, or as a more accurate vectorial polarization term $-\alpha_{\text{He}}\vec{E}_i^2/2$ on each helium atom i , \vec{E}_i being the local electric field created by the sodium ion. In both contributions, $\alpha_{\text{Xe}} = 4.010 \text{ \AA}^3$ and $\alpha_{\text{He}} = 0.205 \text{ \AA}^3$ denote the isotropic atomic polarizabilities of the neutral xenon and helium atoms, respectively. After ionization of the xenon atom, we set a simple Coulombic repulsion between the two ions, and the electric field \vec{E}_i on each helium atom now incorporates the contribution of the xenon ion as well. Keeping the isotropic polarizabilities as fixed parameters, all LJ parameters were adjusted to reproduce the relevant pair interactions. They are tabulated as Supplementary Electronic Material, together with references to the original data used to fit these interactions, and are illustrated in Fig. S1. Other computational details of the present simulations are also provided as Supplementary material.

Unsurprisingly, and owing to the highly polarizable character of the heavy xenon element, the Na^+Xe non-covalent complex is the most strongly bound of all pairs involved in this experimental situation, reaching almost 0.3 eV, to be compared with the few meVs of all neutral pairs, and a few tens of meV for other ionic pairs $\text{Na}^+\text{-He}$ and $\text{Xe}^+\text{-He}$. In neutral state, Na-Xe is also quite more strongly bound than any of the pairs involving helium, but this attraction is not sufficient to bring the two neutral impurities in contact with each other during the initial equilibration period, a result that is consistent with earlier TD-DFT simulations of comparable systems.²⁰

The formation of a helium shell around the sodium ion was monitored in the RPMD simulations by a simple measure of its coordination number $\langle N_C \rangle$ averaged over polymer beads through appropriate cut-off functions,

$$N_c[\mathbf{R}(t)] = \sum_{i \in \text{HND}} f_c(r_{\text{Na-He}}^{(i)}), \quad (1)$$

where $\mathbf{R}(t)$ denotes the set of Cartesian coordinates of the $\text{Na}^+\text{Xe@He}_N$ system, $r_{\text{Na-He}}^{(i)}$ the distance between the sodium ion and the i^{th} helium atom, and $f_c(t)$ a function such that $f_c(r < r_1) = 1$, $f_c(r > r_2) = 0$, being interpolated smoothly between those two values using a fifth-order polynomial. Here $r_1 = 3.84 \text{ \AA}$ and $r_2 = 4.11 \text{ \AA}$ were chosen to ensure that a helium atom does not belong to the shell if sodium is still in neutral form. $\langle N_C \rangle$ is sensitive to the first helium shell only and does not measure the total number of helium atoms captured by the ejected ion. Here, the limited statistics of 10 independent trajectories prevents from attempting an accurate determination of the solvation time from the time autocorrelation function associated with $\langle N_C \rangle$, hence we resort to the simple time variations of this direct quantity.

Fig. 1 shows the time variations of the distance between the two impurities, after sodium is ionized at time $t = 0$, and the corresponding coordination number $\langle N_C \rangle$, for the three droplet sizes of 1000, 2000, and 5000 atoms. For He_{1000} droplets, additional simulations were performed without xenon dopant, and Fig. 1 also shows the variations of the average distance between Na^+ and the center of mass of the droplet upon ionization. The results are barely distinguishable from those obtained for the Xe@He_{1000} droplet, indicating that the xenon dopant exerts no significant attraction on the sodium cation at this early stage.

The decrease of the $\text{Na}^+\text{-Xe}$ distance is monotonic but proceeds through two main stages. During the first picosecond, the system adjusts to its new potential energy surface and the distance decreases slowly but quadratically with time, as expected from semiclassical dynamics where the coordinate of interest has no initial velocity. During the subsequent 3–4 ps, the $\text{Na}^+\text{-Xe}$ distance decreases faster and the extent of sinking reaches about 10 \AA , independently of droplet size. Submersion occurs concomitantly with the formation of the solvation shell of 10 helium atoms around the sodium cation, but it is

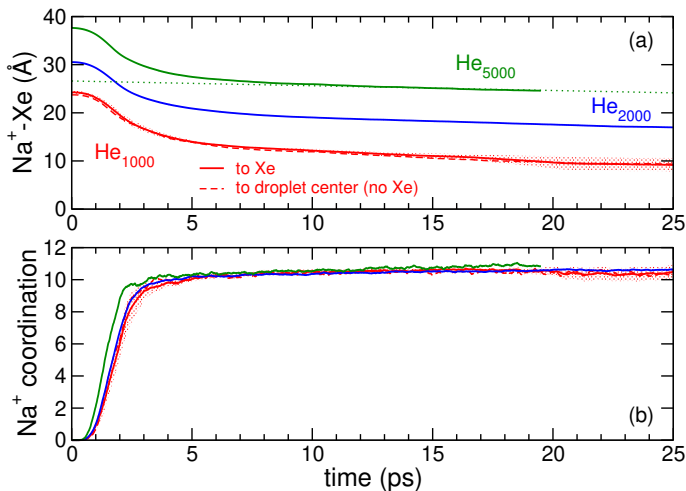


FIG. 1. (a) Average Na⁺-Xe distance, as a function of time after ionization of the sodium impurity, for droplets containing 1000, 2000, and 5000 helium atoms, averaged over 10 independent RPMD trajectories. For He₁₀₀₀, a range of uncertainty is shown from the fluctuations among the 10 independent trajectories. The average distance between Na⁺ and the droplet center is also shown for He₁₀₀₀ droplets lacking the xenon dopant. The dotted line for He₅₀₀₀ suggests a linear extrapolation at longer times; (b) Corresponding variations of the average coordination number of the Na⁺ ion, with fluctuations only shown for the 1000-atom droplets.

interesting to note that the shell is formed prior to the 10 Å submersion, indicating that initially it is the helium atoms that lied in the vicinity of the neutral sodium atom that actually got pulled by the newly formed cation through ion-induced dipole forces, before the ion itself started to sink. This mechanism is also clearly present in the TD-DFT simulations of Albrechtsen *et al.*².

Droplets of a few hundreds of atoms have a radius comparable or smaller to the extent of submersion found here of about 10 Å after 5 ps, and this explains why our earlier RPMD simulations¹¹ found that submersion was complete with the ion reaching the droplet center within about 10 ps. Here, submersion remains incomplete even for He₁₀₀₀ droplets, except for one trajectory in the sample, where the sodium cation meets the xenon dopant about 15-20 ps after ionization, as seen on the increasing fluctuations found for the Na⁺-Xe distance in Fig. 1(a). For this trajectory, the formation of the Na⁺-Xe non-covalent bond leads to a partial decrease in the size of the solvation shell, seen together with increasing statistical fluctuations in Fig. 1(b) at times $t > 15$ ps.

The very slow but steady decrease in the Na⁺-Xe distance can be roughly extrapolated linearly to evaluate the time it would take for complete submersion, that is formation of the Na⁺-Xe non-covalent bond, for all droplet sizes simulated here. Employing the same linear slope extracted for the 5000-atom droplet highlighted with a dotted line in Fig. 1(a), we find times of 70, 100, and 165 picoseconds for He₁₀₀₀, He₂₀₀₀, and He₅₀₀₀, respectively.

More generally, for an arbitrary He_N droplet, the same procedure can be used to predict that the submersion time should vary approximately as $t_s \simeq t_0 + \alpha N^{1/3}$, with fitted parameters $t_0 = -71.25$ ps and $\alpha = 13.89$ ps.

The dynamics following the second ionization of the xenon dopant is next examined. Fig. 2 shows essentially the same properties as Fig. 1, but for the 1000-atom droplets only and for different values of the time delay δt between ionization of the two impurities, $\delta t = 0, 0.5, 1, 2, 5,$ and 10 ps. Under the conditions of simultaneous

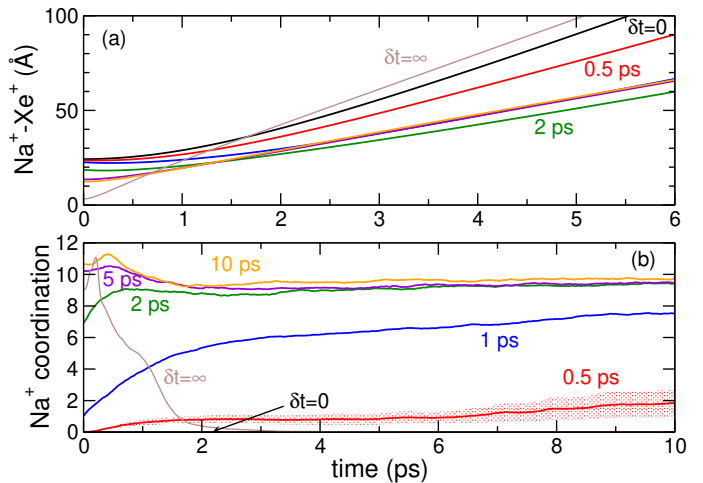


FIG. 2. (a) Average distance between the sodium and xenon ions in He₁₀₀₀ droplets, as a function of time after the xenon dopant was ionized with a delay of δt after the sodium atom; (b) Corresponding variations of the coordination number of the Na⁺ ion. A delay time of ∞ means that the system was prepared as the fully solvated Na⁺Xe complex at equilibrium.

ionizations ($\delta t = 0$), no helium atom is captured by the ejected sodium ion, only a minor fraction ($\langle N_c \rangle \sim 0.1$) being noticed about 1-2 ps after this double ionization, indicating that for one trajectory only, one helium atom had the time to get pulled close enough to the sodium cation before this ion was finally ejected, naked. If the xenon atom is ionized 0.5 ps after the sodium atom, a few helium atoms are definitely captured, but the statistical fluctuations in the coordination number of Fig. 2(b) are quite significant, indicating a peculiar mechanism involving delayed capture. Some example trajectories, illustrated in Fig. S2 (Multimedia available online) of the electronic Supplementary Material, show that for this specific size and at this specific delay time the Coulomb repulsive force balances the attractive solvation (polarization) force originating from the neighboring helium atoms, in such a way that the cation remains in the vicinity of the droplet, without sinking significantly [by less than 0.1 Å, see Fig. 1(a)] but staying long enough for the nearest helium atoms to be pulled towards the cation, still as this ion has turned back and begun its ejection process.

This explains the complex, two-stage behavior in the time variations found for the coordination number at this

droplet size. As the xenon atom is ionized at longer time delays, the sodium cation is able to coat itself with more solvent atoms before being ejected, the full coordination shell of about 10 atoms being formed already after 2 ps.

It is interesting to compare the above situation of finite time delays to the asymptotic case of an initially fully submerged cation. For this problem, additional equilibrium PIMD simulations were performed for the Na^+Xe non-covalent complex embedded inside the helium droplet. The corresponding post-ionization dynamics is referred to as $\delta t = \infty$ in Fig. 2. Quite strikingly, under such assumption the sodium cation is ejected from the droplet in a couple of picoseconds so strongly that any attached solvent atom is vaporized.

In the larger He_{5000} droplets the mechanisms of Coulomb ejection are much softer, as seen in Fig. 3 where the same properties are represented for the same time delays. In particular, even for $\delta t = 0$ the attenuation

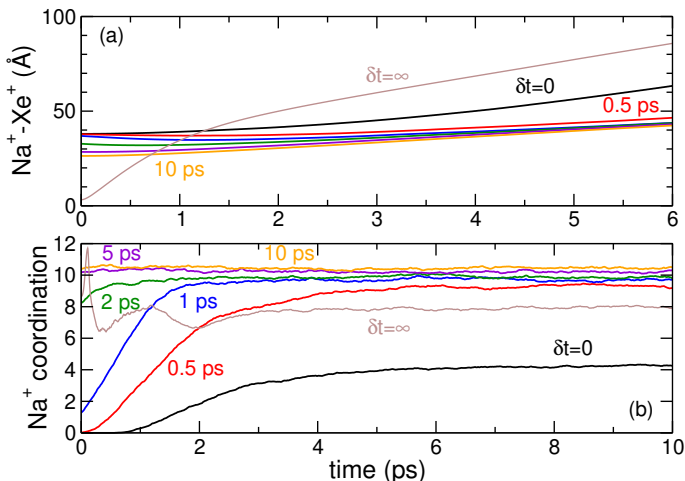


FIG. 3. (a) Average distance between the sodium and xenon ions in He_{5000} droplets, as a function of time after the xenon dopant was ionized with a delay of δt after the sodium atom; (b) Corresponding variations of the coordination number of the Na^+ ion. A delay time of ∞ means that the system was prepared as the fully solvated Na^+Xe complex at equilibrium.

of the Coulomb repulsion relative to the He_{1000} droplet, caused by the larger distance between the two impurities (38 \AA versus 24 \AA), leaves far more time for the sodium cation to capture helium atoms, non-monotonic effects being no longer found for $\delta t = 0.5$ ps (see Fig. S2 in Supplementary Material). Even under the full submersion asymptotic conditions of $\delta t = \infty$, the sodium cation still manages to travel across the droplet and be ejected with a partially filled solvation shell of 8 atoms in average.

Comparing now with the experimental measurements of Ref. 2, the number of helium atoms carried with the ejected sodium cation appears to agree reasonably well for the He_{5000} droplet, but is definitely too small for He_{1000} , which we interpret as reflecting the excessively strong Coulomb repulsion in this smaller droplet: due to the smaller droplet size, the impulse felt by the sodium

cation upon xenon ionization is about 2.5 times stronger than in He_{5000} .

Even with limited statistics, our results can be compared to the experimental measurements, and Fig. 4(a) shows the distributions of the numbers of helium atoms carried by the sodium cation 20 ps after ionization of the xenon atom in He_{5000} droplets and for increasing time delays δt . This number was obtained by partitioning the atoms into various fragments, defined according to a simple connectivity criterion with a cut-off distance of 7 \AA , distances being measured between centroids. While the coordination number only accounts for the first solvation shell around the cation, the total number of helium atoms attached to the cation can thus be much larger. For finite time delays, the fragment size distributions are

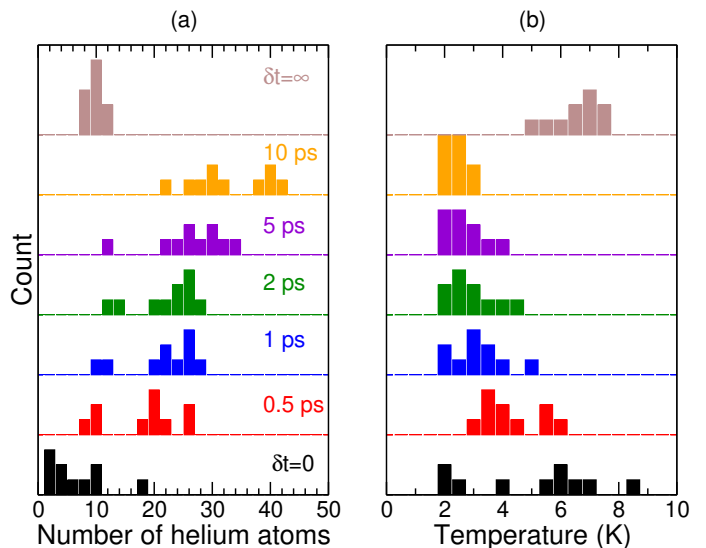


FIG. 4. (a) Distributions of the number of helium atoms carried by the ejected sodium ion in contact with He_{5000} droplets, 20 ps after the xenon dopant was ionized, for different delay times δt between the successive ionizations of both impurities; (b) Distributions of the corresponding temperatures of these fragments.

relatively broad and vary towards increasing values with increasing δt . In contrast, the helium atoms carried away by the ejected sodium cation initially in contact with a xenon atom are fewer and less broadly distributed. The distributions found in the present simulations somewhat overestimate those measured in the experiment.² To solve this discrepancy, we have extended the RPMD trajectories to the ejected fragments Na^+He_p alone and let them evolve for 10 more picoseconds, initially removing the overall linear momentum. A vibrational temperature could thus be estimated from the excess kinetic energy, and the corresponding statistical distributions are shown in Fig. 4(b).

The temperatures estimated for the fragments are notably high and increase with decreasing time delays, but are also significant in the asymptotic limit $\delta t = \infty$. In both cases, high temperatures indicate a solvation shell

that was still not equilibrated 20 ps after xenon ionization, either because it results from sticking collisions to the departing cation (short δt), or because it originates from the violent ejection of the cation through the droplet, dragging with it only a limited number of vibrationally excited solvent atoms. For fragments larger than a dozen atoms, the outer helium atoms that are not tightly bound to the sodium cation are particularly prone to statistical evaporation and we anticipate that smaller fragments would be observed after the experimental time scale of several hundreds of ps, in closer agreement with the measurements but also the classical MD simulations reported in Ref. 2. Besides the ejection of the sodium cation and its flock of helium atoms, the droplet relaxes by a number of other mechanisms that operate at short (rearrangement of the solvation shell), intermediate (evaporation of individual helium atoms from the droplet), or longer times (recoil motion of the xenon cation inside the droplet). In the Supplementary Material (Fig. S3), the two first aspects are scrutinized in more details.

In conclusion, the picture emerging from our path-integral simulations appears to be rather faithful to the experiment carried by Stapelfeldt and coworkers.² By reproducing its main features, our modeling shows that the fragments size distributions are not only a signature of cation solvation itself, but also of the size of the host droplet. The superfluid character of the droplet, which may break down in the vicinity of the newly formed ions,²¹ is not a required property although it is naturally expected to play a role in the ionic dynamics and the propensity of the ejected cation to keep or release helium atoms. It should also play a role in the possible oscillatory motion that could occur at longer times,⁹ although the formation of the rather strongly bound Na^+Xe complex, predicted here to occur after hundreds of picoseconds, should be a further major source of energy dissipation in the system.

The nature of the alkali element should also influence the fragment distribution, and possibly the rate at which solvent atoms are captured,¹⁰ at least through the different equilibrium distances its neutral atom lies from the droplet before ionization, as well as different solvation shells it can accommodate. This will be the object of future efforts.

SUPPLEMENTARY MATERIAL

Details of the interaction potentials and of the PIMD and RPMD simulations; enhanced discussion about two-stage helium capture and energy dissipation; selected animations.

- ¹Y. Marcus, *Ions in solution and their solvation*, John Wiley & Sons, Hoboken, 2015.
- ²S. H. Albrechtsen, C. A. Schouder, A. V. Muñoz, J. K. Christensen, C. Engelbrecht Petersen, M. Pí, M. Barranco and H. Stapelfeldt, *Nature (London)* **623**, 319 (2023).
- ³S. Goyal, D. L. Schutt, and G. Scoles, *Phys. Rev. Lett.* **69**, 933 (1992).
- ⁴J. P. Toennies and A. F. Vilesov, *Angew. Chem. Int. Ed.* **43**, 2522 (2004).
- ⁵M. Y. Choi, G. E. Douberly, T. M. Falconer, W. K. Lewis, C. M. Lindsay, J. M. Merrit, P. L. Stiles and R. E. Miller, *Int. Rev. Phys. Chem.* **25**, 15 (2006).
- ⁶J. Tiggesbäumker and F. Stienkemeier, *Phys. Chem. Chem. Phys.* **9**, 4748 (2007).
- ⁷A. Leal, D. Mateo, A. Hernando, M. Pí, M. Barranco, A. Ponti, F. Cargnoni, and M. Drabbels, *Phys. Rev. B* **90**, 224518 (2014).
- ⁸F. Dalfovo, A. Lastri, L. Pricauptenko, S. Stringari, and J. Treiner, *Phys. Rev. B* **52**, 1193 (1995).
- ⁹D. Mateo, A. Leal, A. Hernando, M. Barranco, M. Pí, F. Cargnoni, M. Mella, X. Zhang, and M. Drabbels, *J. Chem. Phys.* **140**, 131101 (2014).
- ¹⁰E. García-Alfonso, M. Barranco, N. Halberstadt, and M. Pí, *J. Chem. Phys.* **160**, 164308 (2024).
- ¹¹F. Calvo, *Submersion kinetics of ionized impurities into helium droplets by ring-polymer molecular dynamics simulations*, in *Clusters: Structure, Bonding and Reactivity*, Edited by M. T. Nguyen and B. Kiran, Springer Series on Challenges and Advances in Computational Chemistry and Physics 23, Springer, Berlin, 2017.
- ¹²I. R. Craig and D. E. Manolopoulos, *J. Chem. Phys.* **121**, 3368 (2004).
- ¹³J. O. Richardson and S. C. Althorpe, *J. Chem. Phys.* **131**, 214106 (2009).
- ¹⁴A. R. Menzeleev and T. F. Miller, III, *J. Chem. Phys.* **132**, 034106 (2010).
- ¹⁵T. J. H. Hele and S. C. Althorpe, *J. Chem. Phys.* **138**, 084108 (2013).
- ¹⁶R. Welsch, K. Song, Q. Schi, S. C. Althorpe, and T. F. Miller, III, *J. Chem. Phys.* **145**, 204118 (2016).
- ¹⁷B. Hirshberg, V. Rizzi, and M. Parrinello, *Proc. Natl. Acad. Sci. U. S. A.* **116** 21445-21449 (2019).
- ¹⁸F. Briec, C. Schran, F. Uhl, H. Forbert, and D. Marx, *J. Chem. Phys.* **152**, 210901 (2020).
- ¹⁹F. Calvo, C. Falvo, and P. Parneix, *J. Phys. Chem. A* **118**, 5427 (2014).
- ²⁰J. Poms, A. W. Hauser, and W. E. Ernst, *Phys. Chem. Chem. Phys.* **14**, 15158 (2012).
- ²¹T. González-Lezana, O. Echt, M. Gatchell, M. Bartolomei, J. Campos-Martínez, and P. Scheier, *Int. Rev. Phys. Chem.* **39**, 465 (2020).